Signal Detection with Belief Propagation in Faster-than-Nyquist Signaling

Kotaro Kihara, Toshihiko Nishimura, Takeo Ohgane, and Yasutaka Ogawa
Graduate School of Information Science and Technology, Hokkaido University
Kita 14 Nishi 9, Kita-ku, Sapporo, Hokkaido, 060-0814 Japan
Email: k_kihara@m-icl.ist.hokudai.ac.jp, {nishim, ohgane, ogawa}@ist.hokudai.ac.jp

***Abstract*—Faster-than-Nyquist (FTN) signaling is one of the approaches that improve spectrum efficiency by transmitting symbols faster than the Nyquist rate. However, it suffers from inter-carrier interference (ICI) and inter-block interference (IBI). Thus, the ICI and IBI canceller is needed at a receiver. In this paper, signal detection based on belief propagation (BP) is applied to FTN symbol detection. The BP algorithm provides very high performance in signal detection with large scale random factor graphs. However, when we apply the BP algorithm to the FTN signal detection, the factor graph has many short loops locally, and randomness cannot be found in the edge strength distribution. Thus, proper convergence is not always expected. To improve the convergence performance in such an environment, we propose a technique to scale *a posteriori* LLR values before channel decoding. The simulation results show that the error floor is significantly reduced by this LLR scaling.**

I. Introduction

With the rapid spread of communication terminals such as smartphones, it is expected that the traffic of the radio access becomes more than 1,000 times in 2020 than that in 2010 [1]. In order to cope with rapidly-increasing traffic, dramatic improvement in both spectrum efficiency and system throughput is required. In recent years, non-orthogonal multiple access has attracted attention [2], [3] as an approach that can efficiently perform user-scheduling by allowing inter-user interference.

OFDM-based faster-than-nyquist (FTN) is one of the other techniques utilizing non-orthogonality [4], [5]. FTN signaling improves spectrum efficiency by transmitting symbols faster than the Nyquist rate at the expense of inter-carrier interference (ICI) and inter-block interference (IBI). Thus, it is necessary to remove the ICI and IBI at the receiver using an interference canceller.

The similar situation can be seen in signal detection in MIMO systems where inter-stream interference exists. Typical detection techniques are linear spatial filtering, soft interference canceller, and maximum likelihood detection. Recently, in addition to these techniques, signal detection based on a belief propagation (BP) algorithm has been studied in large MIMO systems [6]–[9]. The BP-based detection is a lightweight technique and achieves almost ideal performance when the number of antennas is large enough and the channel correlation is reasonably low [8]. However, the convergence performance of BP generally degrades severely in a bad-conditioned factor graph. Then, other helper techniques such as LLR damping [6], [10] and LLR scaling [11] are needed.

When the BP-based detection is applied to the FTN signal detection, high detection performance cannot be expected because the factor graph has many localized short loops having similar edge strengths as described later. Therefore, it is expected that the BP-based FTN signal detection is a challenge to confirm the capability of BP algorithm. In this paper, we consider to apply the BP-based detection and propose a new helper technique for performance improvement. The rest of the paper is organized as follows. FTN signaling is summarized in Section II. In Section III, signal detection based on the BP algorithm is described. Section IV shows the performance evaluation. Finally, the paper is concluded in Section V.

II. FTN Signaling

First, we describe FTN symbol construction from OFDM symbols. This helps understanding our interference canceller in the later part of this paper. An OFDM symbol sequence is expressed as

$$s_{\mathrm{OFDM}}(t) = \sum_{\ell=-\infty}^{\infty} \sum_{k=0}^{M-1} x_{k,\ell}\, u\big(t-\ell T\big) e^{j2\pi kFt}, \tag{1}$$

where $x_{k,\ell}$ is the data symbol, which is taken from a finite complex alphabet constellation, at the kth subcarrier of the ℓth symbol timing, M is the number of subcarriers, T is the symbol length, F denotes the subcarrier interval, and $u(t)$ represents a pulse waveform. The subcarriers are orthogonal to each other since the Nyquist criterion is satisfied by setting $FT = 1$.

An FTN symbol sequence can be expressed similarly as

$$s_{\mathrm{FTN}}(t) = \sum_{\ell=-\infty}^{\infty} \sum_{k=0}^{M-1} x_{k,\ell}\, v(t-\ell\eta T) e^{j2\pi kFt}, \tag{2}$$

where $v(t)$ is a different pulse waveform. Note that the symbol length is shortened to ηT $(0 < \eta < 1)$ under the same subcarrier interval condition, i.e., $\eta TF < 1$. Thus, the Nyquist criterion is no longer satisfied. This destroys the subcarrier orthogonality and yields an ICI.

Here, let us map each FTN data symbol component to OFDM data symbols. As described above, there is the ICI. In addition, the pulse waveform difference between $u(t)$ and $v(t)$ causes an inter-block interference. Thus, several FTN data symbols are projected on one OFDM data symbol.

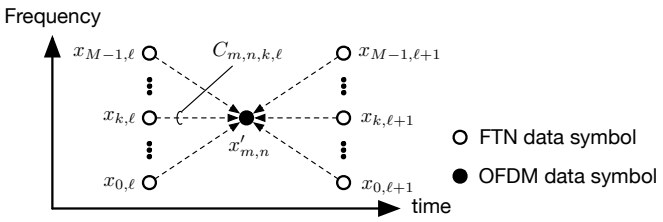

Fig. 1. Illustration of FTN symbols projected on an OFDM symbol.

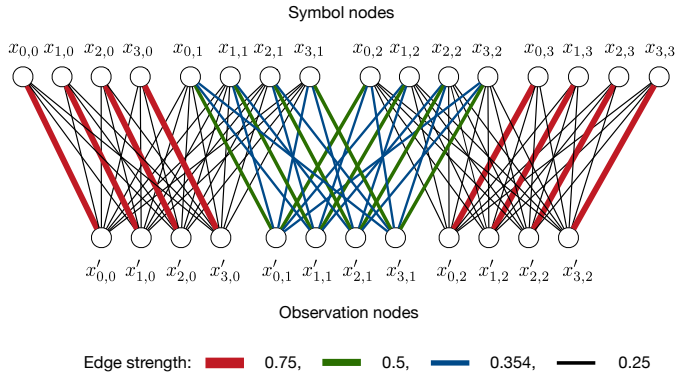

Fig. 2. Factor graph expression for FTN data symbols to be estimated and observed OFDM data symbols.

In this paper, we assume rectangular pulse shapes for $u(t)$ and $v(t)$. The rectangular pulse cannot localize the range of ICI whereas it minimizes the range of IBI. Specifically, all subcarriers in the frequency domain but only two symbols at most in the time domain interfere each other. Thus, we can easily control the number of FTN data symbols projected on one OFDM data symbol by changing the number of subcarriers. Since $u(t)$ or $v(t)$ take the value of 1 within the time of 0 to T or ηT, and 0 otherwise, we can express as follows

$$u\big(t-nT\big)e^{j2\pi mFt} = U_{m,n}(t) \tag{3}$$
$$v\big(t-n\eta T\big)e^{j2\pi mFt} = V_{m,n}(t). \tag{4}$$

Then, the FTN symbol sequence given by (2) can be rewritten as

$$s_{\mathrm{FTN}}(t) = \sum_{\ell=-\infty}^{\infty}\sum_{k=0}^{M-1} x_{k,\ell}\, V_{k,\ell}(t). \tag{5}$$

Mapping this sequence to an OFDM symbol sequence, we can further rewrite the above equation as

$$s_{\mathrm{FTN}}(t) = \sum_{n=-\infty}^{\infty}\sum_{m=0}^{M-1} x'_{m,n}\, U_{m,n}(t), \tag{6}$$

where

$$x'_{m,n} = \sum_{k}\sum_{\ell} C_{m,n,k,\ell} x_{k,\ell}, \tag{7}$$

and $C_{m,n,k,\ell}$ is the projection coefficient of the FTN data symbol at the kth subcarrier of the ℓth symbol timing to the OFDM data symbol at the mth subcarrier of the nth symbol timing, as shown in Fig. 1.

The above formulation does not consider a guard interval (GI). In actual situations, we first map FTN symbols to OFDM symbols. These symbols are followed by IFFT with the OFDM symbol interval, and finally a GI is added [4].

III. Interference Cancellation Based on BP

A. Detection Concept and Factor Graph Expression

The OFDM data symbol after removing the GI from the received FTN symbol sequence and performing the FFT is expressed as

$$x'_{m,n} = \sum_{k}\sum_{\ell} h_m C_{m,n,k,\ell} x_{k,\ell} + z_{m,n}, \tag{8}$$

where h_m is the channel coefficient at the mth subcarrier, and $z_{m,n}$ is a white Gaussian noise. For the sake of simplicity, we assume the maximum time delay of the multipath channel is not greater than the GI.

Our problem is to estimate the transmitted FTN data symbol $x_{k,\ell}$ from the observation $x'_{m,n}$. This can be expressed by a factor graph as shown in Fig. 2. In this figure, we assume 4 subcarriers and 4 FTN symbols with $\eta = 0.75$ as a simple example. The observation nodes in Fig. 2 correspond to the observed OFDM data symbols, and the symbol nodes correspond to the FTN data symbols to be estimated. The edge exists only when the projection coefficient $C_{m,n,k,\ell}$ exits. We can see that edge distribution is localized and that the edge strength, i.e., the projection coefficient takes a constant value at each local region. Actually, there are only 4 different coefficients from 0.25 to 0.75 except zero. Considering many loops in the factor graph and regularity in the edge strength, we may say that the estimation using BP becomes very severe.

B. LLR Update at Observation Nodes

The received OFDM data symbol $x'_{m,n}$ given by (8) can be rewritten as follows when we focus on a certain FTN data symbol $x_{i,j}$:

$$x'_{m,n} = h_m C_{m,n,i,j} x_{i,j} + \sum_{k\neq i}\sum_{\ell\neq j} h_m C_{m,n,k,\ell} x_{k,\ell} + z_{m,n}, \tag{9}$$

where the first term of the righthand side is the signal component of interest, and the second term is the interference from neighboring symbols.

Here, let us consider to estimate a belief of $x_{i,j}$ from $x'_{m,n}$. This corresponds to generating a message to the $(i,\, j)$th symbol node from the $(m,\, n)$th observation node. Equation (9) can be rewritten as

$$h_m C_{m,n,i,j} x_{i,j} = x'_{m,n} - \sum_{k\neq i}\sum_{\ell\neq j} h_m C_{m,n,k,\ell} x_{k,\ell} - z_{m,n}. \tag{10}$$

Clearly, estimating the belief of $x_{i,j}$ from $x'_{m,n}$ requires marginalization of other beliefs of $x_{k,\ell}$. To reduce the cal-

culation complexity, we apply a soft canceller instead of the marginalization.

As a first step, a soft replica $\hat{x}_{k,\ell}$ is calculated from the belief (the extrinsic LLR value) passed from the (k, ℓ)th symbol node. Then, the signal of which ICI and IBI are partly removed is expressed as

$$\tilde{x'}_{m,n} = x'_{m,n} - \sum_{k \neq i} \sum_{\ell \neq j} h_m C_{m,n,k,\ell} \hat{x}_{k,\ell}. \tag{11}$$

In general, in early iteration stages, the replicas are not perfectly reconstructed, ant thus some interference components still remain in $\tilde{x'}_{m,n}$. These are approximately regarded as Gaussian-distributed random values [7]. Each variance (interference power) is calculated from the difference between the expected value of soft replica's power and the data symbol power. After replacing the noise power by a sum of the noise power and residual interference power, the bth bit's LLR of $x_{i,j}$ can be estimated by

$$\alpha^{(b)}_{i,j \leftarrow m,n} = \log \frac{p\left(\tilde{x'}_{m,n} | x^{(b)}_{i,j} = 1\right)}{p\left(\tilde{x'}_{m,n} | x^{(b)}_{i,j} = 0\right)}, \tag{12}$$

where $x^{(b)}_{i,j}$ is the bth bit value of $x_{i,j}$. This process is repeated for all (i, j) combinations, and these LLR values are passed to corresponding symbol nodes.

C. LLR Update at Symbol Nodes

Let us describe the LLR update at the (i, j)th symbol node. At first, *a posteriori* LLR of the bth bit of $x_{i,j}$ is calculated by a sum of LLR values passed from the observation nodes connected by edges as

$$\gamma^{(b)}_{i,j} = \sum_{m,n} \alpha^{(b)}_{i,j \leftarrow m,n}. \tag{13}$$

When channel coding is applied, this *a posteriori* LLR is used as an input of the channel decoder and replaced by the output of the decoder. The final decision is made by this *a posteriori* LLR. The extrinsic LLR value passed to the (m, n)th observation node is obtained by subtracting the LLR value passed from corresponding observation node as

$$\beta^{(b)}_{m,n \leftarrow i,j} = \gamma^{(b)}_{i,j} - \alpha^{(b)}_{i,j \leftarrow m,n}. \tag{14}$$

This process is repeated for all the (m, n) combinations, and these LLR values are passed to the corresponding observation nodes. The initial value of the extrinsic LLR $\beta^{(b)}_{m,n \leftarrow i,j}$ in the observation node is set to 0. Thus, the soft replica becomes 0 at the first iteration.

D. Problems in Factor Graph of FTN

The BP algorithm is a method of improving the reliability of the *a posteriori* LLR by repeatedly exchanging the reliability information between the symbol nodes and the observation nodes. It is known that it works well in the case of LDPC decoder where edges are sparsely distributed. When the factor graph has short loops, the convergence is not guaranteed generally. However, in a massive MIMO environment where many short loops exist in the factor graph, the BP algorithm works well because the edge strength distributes randomly [8].

In the factor graph of FTN, there are many short loops but the edge strength takes one of a few limited values. The edge strength variation increases with the number of subcarriers under the assumption of rectangular pulse shape. Therefore, when the number of subcarriers is too small, it is expected that an influence of short loops increases. In addition, the edges are connected very locally as shown in Fig. 2. It means that nodes providing beliefs are limited in the local region. In other words, a wide-range exchange of beliefs cannot be expected. Thus, we need to take some measures to improve the convergence performance in such a severe-conditioned factor graph.

E. LLR Damping

When the LLR values are not appropriately converged, LLR oscillation is seen frequently [12]. Therefore, reducing such oscillation is expected to improve the convergence performance. A simple way to prevent oscillation is damping [6], [10] which is an exponential average of past reliabilities. Damped LLR values change gradually. Therefore, the oscillation may be prevented. We can damp LLR values at either side of the factor graph. In the paper, we apply the damping at the observation nodes. The LLR values at the (m, n)th observation nodes passed to the (i, j)th symbol nodes are damped as

$$\hat{\alpha}^{(b)}_{i,j \leftarrow m,n} = D \hat{\alpha}^{(b)}_{i,j \leftarrow m,n,\text{prev}} + (1 - D) \alpha^{(b)}_{i,j \leftarrow m,n}, \tag{15}$$

where D ($0 \leq D < 1$) is the damping factor, and $\hat{\alpha}^{(b)}_{i,j \leftarrow m,n,\text{prev}}$ is the damped LLR at the previous iteration. The damped LLR $\hat{\alpha}^{(b)}_{i,j \leftarrow m,n}$ is passed to the (i, j)th symbol node instead of $\alpha^{(b)}_{i,j \leftarrow m,n}$. In this paper, with respect to the value of D, the optimum value was empirically determined in terms of the BER performance.

F. LLR Scaling

LLR scaling (multiplying a positive coefficient less than one) is another approach to improve the convergence performance in severe-conditioned factor graphs. There are two different ways for LLR scaling. One is scaling of $\beta^{(b)}_{m,n \leftarrow i,j}$. This suppresses yielding quasi-hard replicas in soft cancellation at the observation nodes. It is reported that this LLR scaling improves the convergence performance in the uncoded case [11].

Another is scaling of $\alpha^{(b)}_{i,j \leftarrow m,n}$. In the coded case, high LLR inputs to the decoder provides much higher LLR outputs. If some of LLR inputs have wrong information, miscorrection with very high LLR may occur. Therefore, reducing the LLR values of decoder inputs is expected to improve the convergence performance. Here, we propose the LLR scaling of $\alpha^{(b)}_{i,j \leftarrow m,n}$ in (12) as follows. The scaling factor should depend on the LLR value $\alpha^{(b)}_{i,j \leftarrow m,n}$ itself. This adjustment can be done by observing the SINR after soft cancellation in

TABLE I
SIMULATION PARAMETERS.

Modulation	OFDM/QPSK
Number of subcarriers	4 or 8
Symbol interval shortening ratio	0.75
GI ratio	0.25
Block length	3 symbols
Number of blocks	10,000,000
Channel statistics	Block Rayleigh fading
Number of waves	2 (4-subcarrier) or 3 (8-subcarrier)
Channel encoding	Recursive systematic convolutional code (constraint length 3, coding rate 1/2)
Channel decoding	Max-Log MAP decoder
LLR scaling parameters	$0.6 \leq c \leq 0.8$ $0.01 < d < 0.11$
Number of iterations in BP	10

(11). We have tested several functions of SINR and selected one as a tentative solution:

$$\rho_{m,n,i,j} = c\,\mathrm{e}^{-d\xi_{m,n,i,j}}, \tag{16}$$

where c and d are certain constants, and $\xi_{m,n,i,j}$ is the SINR value of $\tilde{x'}_{m,n}$ by regarding $x_{i,j}$ as the signal component. In general, $\alpha^{(b)}_{i,j\leftarrow m,n}$ becomes very high at the high SINR. Therefore, we adjusted $\rho_{m,n,i,j}$ to be a smaller coefficient when SINR is higher. The optimum values of c and d were empirically determined by a trade-off between the cliff and error floor level of BER performance. For comparison, we also performed LLR scaling only using SNR in (16). Specifically, the residual interference power is removed from the denominator of $\xi_{m,n,i,j}$.

IV. NUMERICAL EVALUATIONS

A. Simulation Environment

In this paper, we assume FTN transmission based on an OFDM/QPSK modulation scheme using rectangular pulse. The computer simulations on the BP-based detection have been conducted under the conditions as shown in Table I. The number of subcarriers is 4 or 8. The transmission block length is 3 symbols. The subcarrier interval is the same as OFDM whereas the symbol interval is shortened to 0.75. We used a AWGN channel model or a block Rayleigh fading channel model having an equal power delay profile. In fading channels, the numbers of paths were set to 2 and 3 in the 4-subcarrier and 8-subcarrier cases, respectively, according to the GI length. The channel state information is assumed to be perfectly known at the receiver. As a channel code, a recursive systematic convolutional code (constraint length 3 and coding rate 1/2) is used.

B. BER Performance

Figures 3 and 4 show the BER performance of FTN data symbol detection in the AWGN channel. In the paper, we examine the detection performances of BP-based algorithm with or without LLR damping and scaling. As the baseline, we also evaluate the detection performance using a matched filter [1](denoted as "w/o canceller" in the figures).

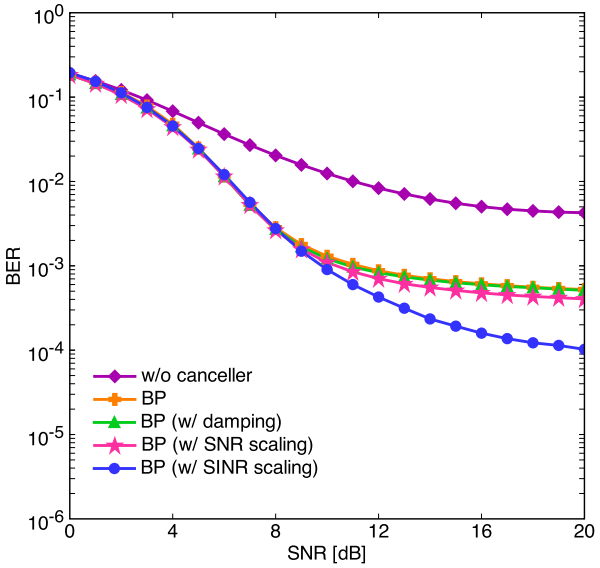

Fig. 3. BER performance of the 4-subcarrier case in the AWGN channel.

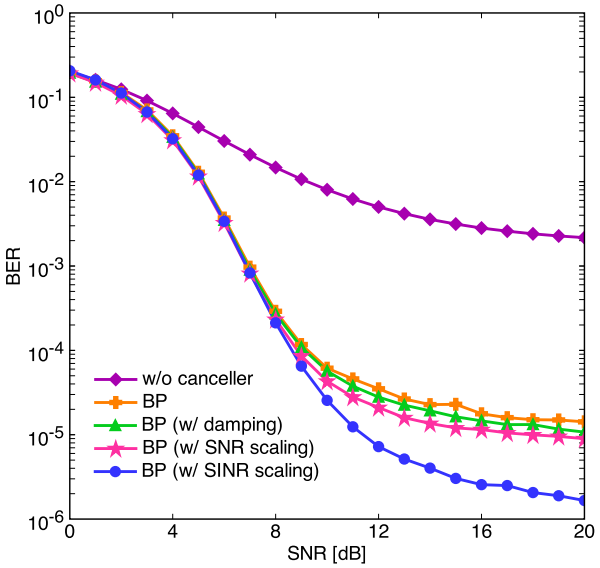

Fig. 4. BER performance of the 8-subcarrier case in the AWGN channel.

It is observed that the BP algorithms reduce the error floor compared with the case without interference cancellation. For the convergence helpers, the SINR-based scaling is most successful in reducing the error floor. It can be said that reducing the input value of the decoder by scaling based on the

[1]In this case, the degrees of freedom are not enough to cancel the interference. Hence, the ZF filtering based on MP generalized inverse matrix is equal to the matched filter.

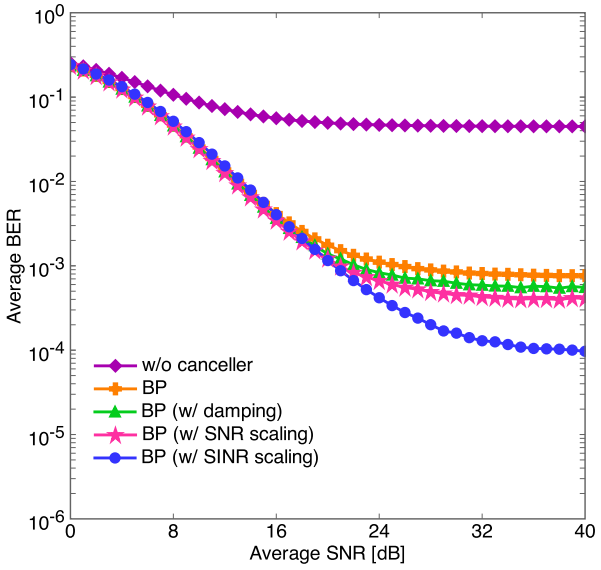

Fig. 5. BER performance of the 4-subcarrier case in the 2-path fading channel.

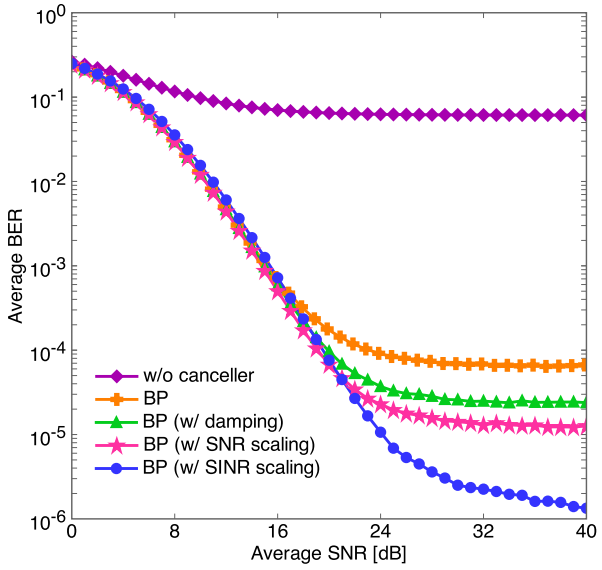

Fig. 6. BER performance of the 8-subcarrier case in the 3-path fading channel.

SINR is very effective for error floor reduction. Furthermore, it can be seen that the convergence performance is further improved when the number of subcarriers is increased to 8. As described before, the edge strength variation increases with the number of subcarriers. Therefore, in the 8-subcarrier case, the short loop effect can be weakened. It is highly expected that the error floor will disappear when the number of subcarrier is much larger.

The BER performance in the fading channel is shown in Figs. 5 and 6. Even in fading environments, the LLR scaling based on SINR shows the best performance and becomes more effective. In the fading channel case, the edge strength is replaced by the multiplication of channel and projection coefficients. Then, a few strong edges appear in the factor graph and become dominant in the message passing. In such a case, some LLR values may be masked by a few big LLR values in (13). The LLR scaling prevents the LLR values from being very large, and thus it is supposed that ill convergence due to LLR masking is reduced by the LLR scaling.

V. Conclusions

In this paper, we applied the BP algorithm to the FTN data symbol detection. The given factor graph has short loops locally and no randomness in the edge strength distribution. Thus, the BER performance was poor when only the BP-based detection is used. In order to improve the performance, we tested LLR damping and proposed a new LLR scaling method. As a result, it has been shown that the LLR scaling based on the SINR reduces the error floor significantly in both AWGN and multipath fading channels.

In the paper, we assumed a simple rectangular pulse for FTN signaling. Because the assumption is unusual, it is needed to check the performance in more general pulse shapes such as Gaussian pulse. In addition, the proposed technique may be applicable to other detection problems. Further studies are needed to investigate these issues.

Acknowledgment

This work was supported by JSPS KAKENHI Grant Number JP15H02252.

References

[1] https://www.nttdocomo.co.jp/corporate/technology/whitepaper_5g/index.html

[2] Y. Saito, Y. Kishiyama, A. Benjebbour, T. Nakamura, L. Anxin, and K. Higuchi, "Non-orthogonal multiple access (NOMA) for cellular future radio access," *Proc. IEEE VTC 2013 Spring*, June. 2013.

[3] K. Higuchi and A. Benjebbour, "Non-orthogonal multiple access (NOMA) with successive interference cancellation for future radio access," *IEICE Trans. Commun.*, vol. E98-B, no. 3, pp. 403-414, Mar. 2015.

[4] D. Dasalukunte, "Multicarrier faster-than-Nyquist signaling transceivers," Ph. D Thesis, Jan. 2012.

[5] M. E. Hefnawy and H. Taoka, "Overview of faster-than-Nyquist for future mobile communication systems," *Proc. IEEE VTC 2013 Spring*, June. 2013.

[6] P. Som, T. Datta, A. Chockalingam, and B. S. Rajan, "Improved large-MIMO detection based on damped belief propagation," *Proc. IEEE ITW 2010*, pp. 1–5, Jan. 2010.

[7] T. Wo and P. A. Hoeher, "Low-complexity Gaussian detection for MIMO systems," *Journal of Electrical and Computer Engineering*, pp. 1–12, Feb. 2010.

[8] W. Fukuda, T. Abiko, T. Nishimura, T. Ohgane, Y. Ogawa, T. Ohwatari, and Y. Kishiyama, "Low-complexity detection based on belief propagation in a massive MIMO system," *Proc. IEEE VTC 2013 Spring*, June. 2013.

[9] A. Chockalingam and B. S. Rajan, *Large MIMO systems*, Cambridge University Press, 2014.

[10] M. Pretti, "A message passing algorithm with damping," *J. Stat. Mech.: Theory and Practice*, Nov. 2005.

[11] T. Takahashi, S. Ibi, and S. Sampei, "On normalization of matched filter belief in GaBP for large MIMO detection," *Proc. IEEE VTC 2016-Fall*, Sep. 2016.

[12] Q. Su and Y. C. Wu, "On convergence conditions of Gaussian belief propagation." *IEEE Trans. Signal Process.*, vol. 63, no. 5, pp. 1144–1155, Mar. 2015.